Mon. Not. R. Astron. Soc. **000**, 000–000 (0000) Printed 7 July 2010 (MN LATEX style file v2.2)

Magneto-elastic oscillations of relativistic stars

Michael Gabler[1,2,3], Pablo Cerdá-Durán[1], José A. Font[2], Ewald Müller[1] and Nikolaos Stergioulas[3]

[1]*Max-Planck-Institut für Astrophysik, Karl-Schwarzschild-Str. 1, 85741 Garching, Germany*
[2]*Departamento de Astronomía y Astrofísica, Universidad de Valencia, 46100 Burjassot (Valencia), Spain*
[3]*Department of Physics, Aristotle University of Thessaloniki, Thessaloniki 54124, Greece*

7 July 2010

ABSTRACT

We discuss results from general-relativistic magnetohydrodynamical simulations of magnetised neutron star models (magnetars) including the effects of an elastic crust. The simulations reveal three distinct regimes: (a) a weak-field limit for magnetic field strengths $B < 5\times10^{13}$ G where purely crustal shear oscillations are recovered, (b) a strong-field limit $B > 10^{15}$G where the magnetic field dominates the dynamics and the resulting quasi-periodic oscillations (QPOs) agree qualitatively with previous work, and (c) an intermediate regime, where purely crustal modes are damped rapidly with increasing magnetic field strength. Due to the presence of a solid crust a polar region exists where the standing-wave condition is significantly modified. As a result, strong QPOs are localised at a substantial angular distance from the pole. The boundary conditions at the base of the crust lead to a reversal in the order of the various families of QPOs. Pure crustal oscillations are strongly absorbed by the Alfvén continuum even for relatively low values of the poloidal magnetic field strength. This excludes torsional, axisymmetric shear modes of the crust as a viable interpretation of observed long-lived QPOs in giant flares of soft-gamma repeaters, if magnetic fields in magnetars are dominated by an axisymmetric dipolar component.

Key words: relativity – MHD – stars: neutron – stars: oscillations – stars: magnetic fields – gamma rays: theory

1 INTRODUCTION

The observation of giant flares in Soft Gamma Repeaters (SGRs; compact objects with very strong magnetic fields or magnetars (Duncan & Thompson 1992)) may open a gateway towards the exciting field of neutron star seismology. In the decaying X-ray tail of two such events, SGR 1900+14 and SGR 1806-20, a number of long-lasting, quasi-periodic oscillations (QPOs) have been observed (see Israel et al. (2005) and Watts & Strohmayer (2007) for recent reviews). Early models interpreted the observed QPO frequencies as directly related to torsional shear oscillations of the solid crust of a neutron star excited during a giant flare event (see Duncan (1998); Strohmayer & Watts (2005); Piro (2005); Sotani et al. (2007); Samuelsson & Andersson (2007), and references therein). Due to the extremely strong magnetic fields present in magnetars, however, a self-consistent model that includes global magnetohydrodynamic (MHD) oscillations interacting with the shear oscillations of the crust is required (Levin (2006), Glampedakis & Andersson (2006), Levin (2007), Lee (2007, 2008)). Using a simplified model, Levin (2007) showed that shear oscillations can be absorbed by a MHD continuum of Alfvén oscillations, while long-lived QPOs may still appear at the turning points or edges of the continuum.

Sotani et al. (2008) and subsequently Cerdá-Durán et al. (2009) (see also Colaiuda et al. (2009)), using a more realistic, general-relativistic MHD model but still ignoring an extended crust, found two families of QPOs related to turning points of the frequency of torsional Alfvén waves near the magnetic pole and inside a region of closed magnetic field lines near the equator. Each QPO family consists of two sub-families differing by their symmetry behaviour with respect to the equatorial plane. This Alfvén QPO model is very attractive, because it reproduces the near-integer-ratios of the observed 30, 92 and 150 Hz frequencies in SGR 1806-20. The results of the numerical simulations agree with a semi-analytic model based on standing waves in the short-wavelength limit (Cerdá-Durán et al. 2009).

The omission of an extended crust in the previous studies of Sotani et al. (2008), Cerdá-Durán et al. (2009), and Colaiuda et al. (2009) can be considered as a limiting case of a very strong magnetic field. For intermediate magnetic field strengths, however, an understanding of magnetar oscillations requires the inclusion of crust-core coupling. In this Letter, we present the first such simulations of coupled, magneto-elastic oscillations. We use a general-relativistic framework, a dipolar magnetic field, and a tabulated equation of state (EOS) for dense matter. The numerical simulations are based on state-of-the-art Riemann solver methods for both

the interior MHD fluid and the crust. Furthermore, we extend the semi-analytic model of Cerdá-Durán et al. (2009) by including a description of crust-core coupling that provides a comparison aiding the interpretation of our numerical results. A recent study by van Hoven & Levin (2010) also takes entanglement of magnetic field lines into account, thereby generalising the toy model of Levin (2007). Some first results on coupled crust-core oscillations also appeared in Kokkotas et al. (2010).

We use units where $c = G = 1$ with c and G being the speed of light and the gravitational constant, respectively. Latin (Greek) indices run from 1 to 3 (0 to 3).

2 THEORETICAL FRAMEWORK

The present study of torsional oscillations of magnetars is based on a numerical integration of the general relativistic MHD equations. As Cerdá-Durán et al. (2009), who considered purely Alfvén oscillations of the fluid core, we simplify the problem by assuming (i) a zero temperature EOS, (ii) axisymmetry, (iii) a purely poloidal magnetic field configuration, (iv) the Cowling approximation, and (v) a spherically symmetric background. Because of assumptions (ii) and (iii) polar oscillations decouple from axial ones in the linear regime. Therefore, we only evolve the φ-component of the evolution variables. We assume a conformally flat metric [1]

$$ds^2 = -\alpha^2 dt^2 + \phi^4 \left(dr^2 + r^2 d\theta^2 + r^2 \sin\theta^2 d\varphi^2 \right) , \qquad (1)$$

where α is the lapse function and ϕ the conformal factor, and consider a stress-energy tensor $T^{\mu\nu}$ of the form

$$\begin{aligned} T^{\mu\nu} &= T^{\mu\nu}_{\rm fluid} + T^{\mu\nu}_{\rm mag} + T^{\mu\nu}_{\rm elas} \\ &= \rho h u^\mu u^\nu + P g^{\mu\nu} + b^2 u^\mu u^\nu + \frac{1}{2} b^2 g^{\mu\nu} - b^\mu b^\nu \\ &\quad -2\mu_{\rm S} \Sigma^{\mu\nu} , \end{aligned} \qquad (2)$$

where ρ is the rest-mass density, h the specific enthalpy, P the isotropic fluid pressure, u^μ the 4-velocity of the fluid, b^μ the magnetic field measured by a co-moving observer (with $b^2 := b^\mu b_\mu$), $\Sigma^{\mu\nu}$ the shear tensor, and $\mu_{\rm S}$ the shear modulus, respectively. The latter is obtained according to Sotani et al. (2007).

The conservation of energy and momentum $\nabla_\nu T^{\mu\nu} = 0$, and the induction equation lead to the following system of evolution equations

$$\frac{1}{\sqrt{-g}} \left(\frac{\partial \sqrt{\gamma} \mathbf{U}}{\partial t} + \frac{\partial \sqrt{-g} \mathbf{F}^i}{\partial x^i} \right) = 0 , \qquad (3)$$

where g and γ are the determinants of the 4-metric and 3-metric, respectively. The two-component state and flux vectors are given by

$$\mathbf{U} = [S_\varphi, B^\varphi] , \qquad (4)$$

$$\mathbf{F}^r = \left[-\frac{b_\varphi B^r}{W} - 2\mu_S \Sigma^r_{\ \varphi}, -v^\varphi B^r \right] , \qquad (5)$$

$$\mathbf{F}^\theta = \left[-\frac{b_\varphi B^\theta}{W} - 2\mu_S \Sigma^\theta_{\ \varphi}, -v^\varphi B^\theta \right] , \qquad (6)$$

where B^i are the magnetic field components as measured by an *Eulerian observer* (Antón et al. 2006), and $W = \alpha u^t$ is the Lorentz factor. The shear tensor $\Sigma^{i\varphi} = 1/2 g^{ii} \xi^\varphi_{\ ,i}$ contains the spatial derivatives (denoted by a comma) of the fluid displacement ξ^φ due to the oscillations, which are related to the fluid 4-velocity according to $\xi^\varphi_{\ ,t} = \alpha v^\varphi = u^\varphi / u^t$, where v^φ is the φ-component of the fluid 3-velocity. Hence, the evolution of the spatial derivatives $\xi^\varphi_{\ ,r}$ and $\xi^\varphi_{\ ,\theta}$ is given by

$$(\xi^\varphi_{\ ,k})_{,t} - (\alpha v^\varphi)_{,k} = 0 \qquad \text{with} \quad k \in \{r, \theta\} . \qquad (7)$$

We also need to provide boundary conditions. At the surface the radial derivative of the displacement has to vanish ($\xi^\varphi_{\ ,r} = 0$), as we assume a continuous traction and vanishing surface currents. At the crust-core interface we demand the continuity of the parallel electric field, which implies a continuous displacement ξ^φ. Together with the continuity of the traction the latter leads to a relation between the radial derivatives of the displacement in the core and in the crust: $\xi^\varphi_{{\rm core},r} = (1+\delta)\, \xi^\varphi_{{\rm crust},r}$ with $\delta = \mu_{\rm S} / (b_r b^r)$.

To construct equilibrium models we can choose between different barotropic equations of state for the core that have to be matched to an EOS of the crust. Here we consider the EOS combination APR + DH (Akmal et al. (1998), Douchin & Haensel (2001)), and a particular magnetar model with a mass of $1.4\, M_\odot$ and a radius $R_{\rm star} = 12.26$ km. In contrast to Sotani et al. (2007) the equilibrium models are computed using the LORENE library (`www.lorene.obspm.fr`).

Our simulation code is an extended version of the GRMHD code presented in Cerdá-Durán et al. (2009). It includes the shear terms as they appear in (2), and the evolution of the displacements (7). The proper working of the MHD part of the code was demonstrated in Cerdá-Durán et al. (2008). To test the extended code we compared its results obtained for two limiting cases, zero magnetic field and zero shear modulus, with those of previous studies. The purely crustal shear oscillations presented in Sotani et al. (2007) are recovered with an agreement of 1%, and the Alfvén continuum is obtained naturally as in Cerdá-Durán et al. (2009). Further details on the derivation of the model equations, the numerical methods, and the code tests will be discussed in Gabler et al. (2010).

3 RESULTS

To study the behaviour of coupled crust-core oscillations we perturb the equilibrium stellar model by imposing a velocity perturbation and then follow the time evolution of the system (3) - (7). Unless stated otherwise, we use a grid of 150×100 zones in our simulations covering a domain $[0, R_{\rm star}] \times [0, \pi]$. The angular grid is equidistant, while the radial grid is equidistant only in the crust, where 40 per cent of the zones are located, and coarsens towards the centre of the star. Symmetries are exploited whenever a perturbation is of purely odd or even parity with respect to the equatorial plane. We use the term *damping* in the following to refer to resonant absorption of crustal shear oscillations by the Alfvén continuum of the core (unless we explicitly refer to numerical damping caused by finite-differencing).

Damping of crustal shear modes

We investigated perturbations of different radial extent encompassing only the crust, only the core, or the whole star. Since all three types of perturbations give qualitatively similar results, we focus on whole star perturbations in the following, as this is the most generic case.

[1] This provides a very good approximation as our neutron star models are almost perfectly spherically symmetric except for very small deviations due to the presence of an axisymmetric magnetic field.

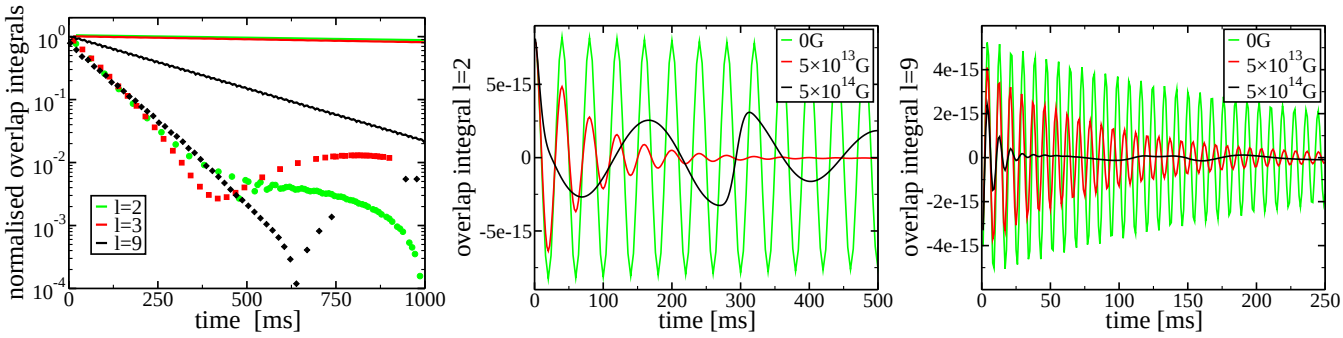

Figure 1. Time evolution of overlap integrals with the eigenmodes of the crust. *Left panel*: Damping of $l = 2, 3$, and 9 initial perturbations due to resonant absorption of the fundamental ($n = 0$) crustal shear mode for a magnetised model with 5×10^{13} G (dots). In the corresponding unmagnetised models (solid lines) only numerical damping occurs which increases with the angular order l of the mode. *Middle panel*: Overlap integrals for the $l = 2$ mode, where resonant absorption of the crustal modes becomes stronger with increasing magnetic field strength. *Right panel*: same as middle panel, but for $l = 9$.

l	2	3	9	10
τ [s] for $B = 0$	5.500	5.070	0.260	0.170
τ [s] for $B = 5 \times 10^{13}$ G	0.072	0.080	0.094	0.100

Table 1. Damping timescales τ due to resonant absorption of crustal shear modes by the Alfvén continuum for various initial perturbation modes l.

We first consider initial perturbations that have a single l-dependence of the corresponding torsional, spherical vector harmonics. To investigate the damping of a single crustal mode we compute *overlap integrals* of the evolved variables with mode eigenfunctions (the latter are found by solving the linear eigenvalue problem for the crustal modes, see Messios et al. (2001); Sotani et al. (2007); Schumaker & Thorne (1983)). Because the eigenmodes of the crust form a complete orthonormal set we can expand any perturbation in terms of the corresponding eigenfunctions. The expansion factors, which provide a measure of how strong each crustal mode contributes to the perturbation, are obtained via the overlap integrals with the eigenfunctions. For more details on this method see Gabler et al. (2009). In the left panel of Fig. 1 we show the maximum (absolute) amplitudes of the overlap integrals for different initial perturbations and for simulations both without magnetic field (solid lines) and with a polar magnetic field of 5×10^{13}G (dots) . In the field-free case the lines represent the *numerical damping* of crustal modes due to finite-differencing. When a magnetic field is present, the damping (now due to resonant absorption) increases with the magnetic field strength.

For all modes, the timescale of resonant absorption is much shorter than that of numerical damping, and the amplitude decreases on a similar timescale (see Tab. 1). After $\sim$ 500 ms, the overlap integrals do no longer sample the crust oscillations, but instead the magneto-elastic oscillations which then dominate the evolution (see below).

The middle and right panels of Fig. 1 show the overlap integrals for $l = 2$ and $l = 9$ modes of the crust as a function of time for different magnetic field strengths, respectively. For $l = 2$ and $B = 5 \times 10^{13}$ G we find almost complete damping of the crustal mode after ~ 0.5 s. For a stronger magnetic field ($B = 5 \times 10^{14}$ G) the crustal mode becomes already damped after less than one oscillation, and only the dominant magneto-elastic oscillations remain. Similar statements hold for the evolution of the $l = 9$ perturbation. However, in that case it takes a few oscillations before the crustal mode is damped, even for $B = 5 \times 10^{14}$ G.

We also analysed a more general initial perturbation consisting of a mixture of $l = 2$ up to $l = 10$ modes, which excites a large number of crustal modes of different angular order l and radial order n. Fig. 2 shows the resulting evolution of the velocity in the crust at $\theta = \pi/4$. For the unmagnetised model low frequency, fundamental ($n = 0$) oscillations can easily be distinguished from higher frequency overtones with $n \geqslant 1$. When increasing the magnetic field to 5×10^{13} G the lower frequency modes are damped on a timescale of $\sim$ 250 ms, whereas the higher frequency overtones survive for a longer time. In the long run, a low frequency ($\sim$ 0.3 Hz) magneto-elastic oscillation dominates. At the largest magnetic field strength shown here, 5×10^{14} G, there is no sign of either low or high frequency crustal modes, the evolution being completely dominated by magneto-elastic oscillations.

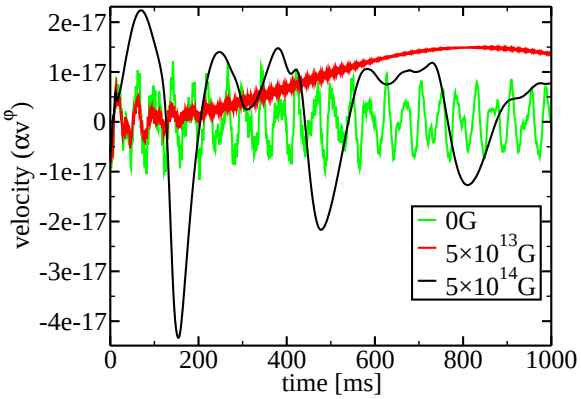

Figure 2. Evolution of αv^{φ} in the crust at $\theta = \pi/4$ for initial data containing a large number of different perturbation modes. For vanishing magnetic field, only crustal modes are excited. For $B = 5 \times 10^{13}$ G the crustal oscillations are strongly damped, and for a ten times stronger magnetic field ($B = 5 \times 10^{14}$ G) magneto-elastic oscillations dominate the evolution from the start.

Long-term QPOs

Besides the damping of crustal modes, we observe long-lasting oscillations in the fluid core of the magnetar. These *long-term QPOs* are identified by local maxima in Fourier space. Let us consider an intermediate magnetic field strength of 4×10^{14} G, where both the magnetic field and the crust influence the dynamics. As in the case without crust (Sotani et al. 2008; Cerdá-Durán et al. 2009) we find two different families of long-term QPOs, as demonstrated in

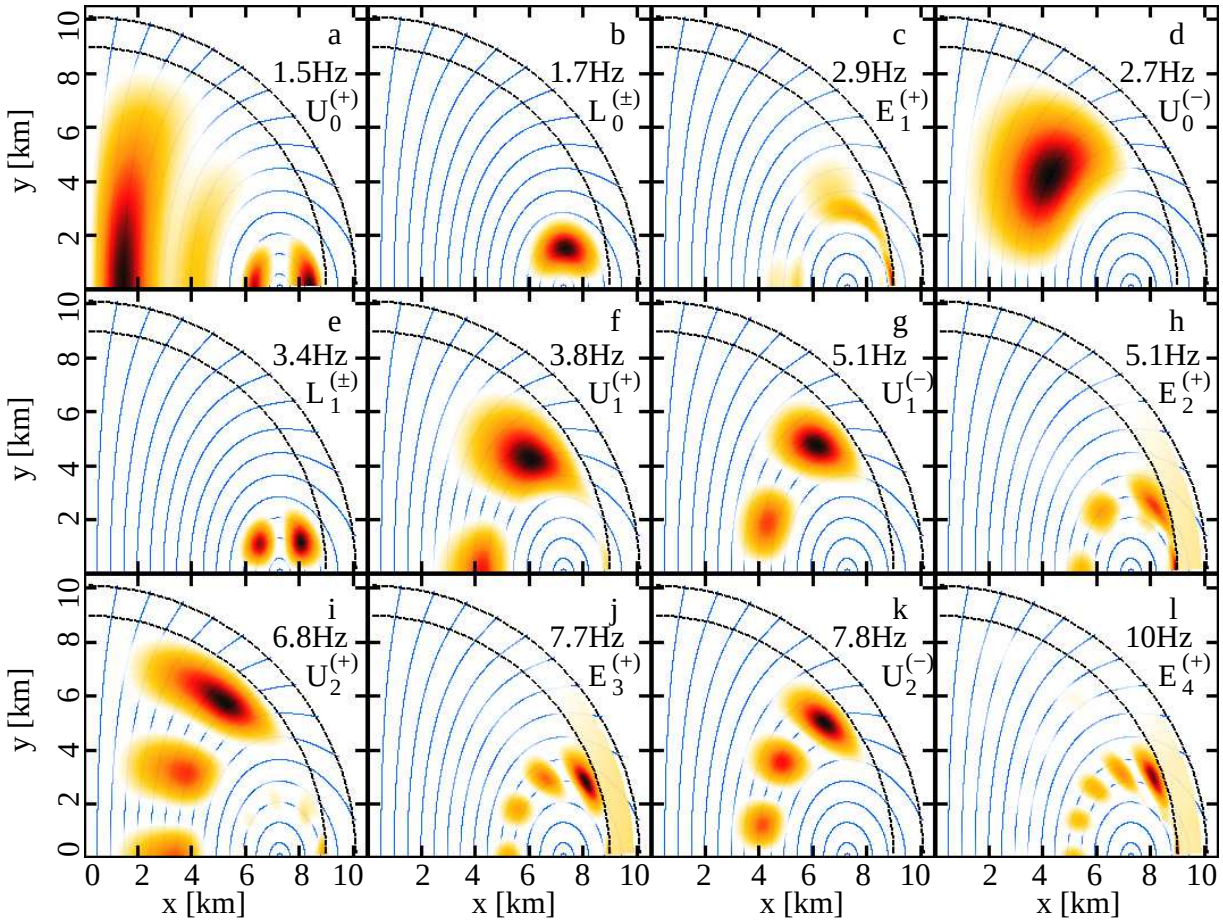

Figure 3. Spatial distribution of Fourier amplitudes at several QPO frequencies. Three different types of QPOs are present: (i) upper QPOs in panels *a, d, f, g, i*, and *k*; (ii) lower QPOs in panels *b* and *e*; (iii) edge QPOs in panels *c, h, j*, and *l*. The two black dashed lines mark the location of the crust, while the blue lines represent magnetic field lines. The colour scale ranges from zero amplitude (white) to maximum amplitude (black).

Fig. 3 which shows the spatial distribution of Fourier amplitudes at several QPO frequencies. The *lower* QPOs ($L_n^{(\pm)}$) are located inside the region of closed field lines, while the *upper* QPOs ($U_n^{(\pm)}$) concentrate along open magnetic field lines closer to the poles. We computed QPOs of either odd $(-)$ or even $(+)$ parity w.r.t. the equatorial plane, which allows for a better identification of QPOs of similar frequency but opposite parity.

The lower QPOs (Fig. 3, panels *b* and *e*) appear to be similar to those found for models without crust, except that they are limited to the region of closed magnetic field lines inside the core. The upper QPOs are influenced by the presence of the crust in several ways. First, they are limited to the fluid region, and become vanishingly small at the base of the crust (Fig. 3, panels *a, d, f, g, i*, and *k*), where they are reflected. This behaviour is similar to that caused by the boundary conditions in Sotani et al. (2008), and differs from that of the pure fluid case considered in Cerdá-Durán et al. (2009). In the latter work the continuous traction boundary condition imposed at the surface of the star resulted in a strong displacement there. Their different behaviour at the base of the crust (w.r.t. the pure fluid case in Cerdá-Durán et al. (2009)) causes a rearrangement of the QPOs. Here, the lowest frequency QPO (panel *a*) is symmetric w.r.t. the equatorial plane (even parity), while it did not exist at all in Cerdá-Durán et al. (2009) and the lowest-frequency QPO has odd parity.

While QPOs are located close to the symmetry axis of the field (polar axis) in models without crust (Sotani et al. 2008; Cerdá-Durán et al. 2009), they are attached to field lines crossing the equator at around 4 km in our models including the crust. Apparently the strong coupling introduced by the crust complicates the oscillatory behaviour of the field lines, such that the interaction between neighbouring polar field lines prevents the QPOs from being established.

Furthermore, we find a new family of QPOs (Fig. 3, panels *c, h, j*, and *l*) connected to the last open field line of the fluid core, each member representing the lower-frequency edge of an Alfvén continuum. Their identification as *edge* QPOs ($E_n^{(+)}$) becomes more obvious in Fig. 4 where we show the amplitude of the Fourier transform averaged along individual magnetic field lines, in a frequency vs. magnetic field line plot, in comparison to the continuum of frequencies obtained with the semi-analytic model of Cerdá-Durán et al. (2009) (solid lines – adapted here to extend up to the base of the crust with reflecting boundary conditions). For even parity modes (right panel) there are large amplitudes in the averaged Fourier transform at around 5.5 km for 2.5, 5.0, and 7.5 Hz, respectively. Those positions coincide approximately with lower-frequency edges of those parts of the continuum that do not connect to the continuum of the closed field lines. QPOs at similar locations were also identified in simulations by Colaiuda et al. (2009) without a crust.

In Fig. 4 one can also identify the families of lower QPOs (restricted to the region of closed field lines in the fluid core) and upper QPOs (which appear along open field lines, but away from the po-

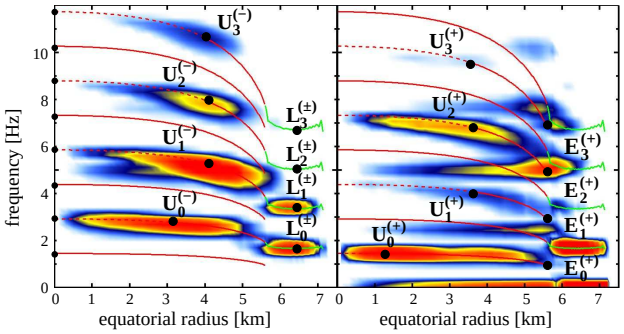

Figure 4. Distribution of the magnitude of the Fourier transform, averaged along individual magnetic field lines, in a frequency vs. magnetic field line plot (magnetic field lines are labeled by the equatorial radius where they cross the equatorial plane). The numerical results agree well with the continuum of frequencies obtained with a semi-analytic model (solid and dashed lines). We indicate the approximate location of the expected QPOs along the continuum by black dots. The *left panel* shows odd-parity and the *right panel* even-parity QPOs. The colour scale ranges from zero (white-blue) to maximum amplitude (orange-red).

lar axis). The region near the polar axis where apparently no stable standing waves can be maintained is displayed with dashed lines. Thus, the upper QPOs are not turning-point QPOs (as was the case in the absence of a crust), but QPOs at the high-frequency edge of a continuum. Notice that the fundamental even-parity QPO is located much closer to the polar axis than any other QPO.

4 DISCUSSION

In this Letter we have presented the first numerical simulations of axisymmetric, torsional Alfvén oscillations in magnetars including an extended crust. In the limit of very strong magnetic fields the results agree with previous studies of Alfvén oscillations in the absence of a solid crust (Sotani et al. 2008; Cerdá-Durán et al. 2009; Colaiuda et al. 2009), while for very weak magnetic fields crustal shear oscillations are recovered. In the intermediate regime 5×10^{13} G to 1×10^{15} G, we find strong resonant absorption of crustal shear modes by the Alfvén continuum of the core, while the Alfvén oscillations are influenced by the shear modulus and become magneto-elastic oscillations.

Long-term QPOs appear to be reflected at the base of the crust leading to a QPO rearrangement with respect to the strong-field limit. For such magnetic field strengths we thus conclude that neither shear modes of the crust nor magneto-elastic QPOs could easily explain the properties of observed QPOs, since the former will be strongly damped, while the latter will be mostly contained within the fluid core. At lower magnetic field field strengths, $B < 5 \times 10^{13}$ G, shear oscillations of the crust may still exist. But in this regime it is unclear which mechanism could cause the giant flare of the SGR during which the QPOs are observed. We also cannot rule out the case that the magnetic field of a magnetar ($B \sim 10^{14} \ldots 10^{15}$ G) is confined to the crust, which may be realised when the core is a type I superconductor. In this case crustal shear modes would not be absorbed by the core. Moreover, it is unclear how the corresponding spectrum would look like, and whether the frequencies of the shear oscillations are unchanged in such a scenario or not.

Regarding magnetic fields penetrating the core of the neutron star, our results favour magnetic field strengths in magnetars larger than $\sim 10^{15}$ G, with dominant Alfvén QPOs extending to the surface of the star, as in Cerdá-Durán et al. (2009) and Colaiuda et al. (2009).

It will be interesting to extend our model by taking into account additional effects, such as the coupling of the interior dynamics to a magnetosphere and the effect of field-line entanglement.

ACKNOWLEDGEMENTS

Work supported by the Collaborative Research Center on Gravitational Wave Astronomy of the Deutsche Forschungsgemeinschaft (DFG SFB/Transregio 7), the Spanish *Ministerio de Educación y Ciencia* (AYA 2007-67626-C03-01) and the European research community Compstar. One of the authors (MG) also acknowledges support through an DAAD exchange grant. The computations were performed on the SGI/Altix3000 computer `Cesar` at the *Servicio de Informática de la Universidad de Valencia*.

REFERENCES

Akmal A., Pandharipande V. R., Ravenhall D. G., 1998, Phys. Rev. C, 58, 1804
Antón L., Zanotti O., Miralles J. A., Martí J. M., Ibáñez J. M., Font J. A., Pons J. A., 2006, ApJ, 637, 296
Cerdá-Durán P., Font J. A., Antón L., Müller E., 2008, A&A, 492, 937
Cerdá-Durán P., Stergioulas N., Font J. A., 2009, MNRAS, 397, 1607
Colaiuda A., Beyer H., Kokkotas K. D., 2009, MNRAS, 396, 1441
Douchin F., Haensel P., 2001, A&A, 380, 151
Duncan R. C., 1998, ApJ, 498, L45+
Duncan R. C., Thompson C., 1992, ApJ, 392, L9
Gabler M., Cerdá-Durán P., Font J., Stergioulas N., 2010, in preparation
Gabler M., Sperhake U., Andersson N., 2009, Phys. Rev. D, 80, 064012
Glampedakis K., Andersson N., 2006, MNRAS, 371, 1311
Israel G. L., Belloni T., Stella L., Rephaeli Y., Gruber D. E., Casella P., Dall'Osso S., Rea N., Persic M., Rothschild R. E., 2005, ApJ, 628, L53
Kokkotas K. D., Gaertig E., Colaiuda A., 2010, Journal of Physics: Conference Series, 222, 012031
Lee U., 2007, MNRAS, 374, 1015
Lee U., 2008, MNRAS, 385, 2069
Levin Y., 2006, MNRAS, 368, L35
Levin Y., 2007, MNRAS, 377, 159
Messios N., Papadopoulos D. B., Stergioulas N., 2001, MNRAS, 328, 1161
Piro A. L., 2005, ApJ, 634, L153
Samuelsson L., Andersson N., 2007, MNRAS, 374, 256
Schumaker B. L., Thorne K. S., 1983, MNRAS, 203, 457
Sotani H., Kokkotas K. D., Stergioulas N., 2007, MNRAS, 375, 261
Sotani H., Kokkotas K. D., Stergioulas N., 2008, MNRAS, 385, L5
Strohmayer T. E., Watts A. L., 2005, ApJ, 632, L111
van Hoven M., Levin Y., 2010, Magnetar Oscillations I: strongly coupled dynamics of the crust and the core, arXiv:1006.0348
Watts A. L., Strohmayer T. E., 2007, Advances in Space Research, 40, 1446